Conformational heterogeneity in closed and open states of the KcsA potassium channel in lipid bicelles

Dorothy M. Kim,[1] Igor Dikiy,[2] Vikrant Upadhyay,[1] David J. Posson,[1,4] David Eliezer,[2,3] and Crina M. Nimigean[1,2,4]

[1]Department of Anesthesiology, [2]Department of Biochemistry, [3]Brain and Mind Research Institute, and [4]Department of Physiology and Biophysics, Weill Cornell Medical College, New York, NY 10065

The process of ion channel gating—opening and closing—involves local and global structural changes in the channel in response to external stimuli. Conformational changes depend on the energetic landscape that underlies the transition between closed and open states, which plays a key role in ion channel gating. For the prokaryotic, pH-gated potassium channel KcsA, closed and open states have been extensively studied using structural and functional methods, but the dynamics within each of these functional states as well as the transition between them is not as well understood. In this study, we used solution nuclear magnetic resonance (NMR) spectroscopy to investigate the conformational transitions within specific functional states of KcsA. We incorporated KcsA channels into lipid bicelles and stabilized them into a closed state by using either phosphatidylcholine lipids, known to favor the closed channel, or mutations designed to trap the channel shut by disulfide cross-linking. A distinct state, consistent with an open channel, was uncovered by the addition of cardiolipin lipids. Using selective amino acid labeling at locations within the channel that are known to move during gating, we observed at least two different slowly interconverting conformational states for both closed and open channels. The pH dependence of these conformations and the predictable disruptions to this dependence observed in mutant channels with altered pH sensing highlight the importance of conformational heterogeneity for KcsA gating.

The Journal of General Physiology

INTRODUCTION

Ion channel gating is a dynamic process involving several coordinated and often poorly understood structural changes within the channel. A complete set of all of the conformations adopted by channels is required to fully understand the complex energetics involved in channel function. Electrophysiological studies report on the functionally closed and open states of a channel but do not provide a structural framework for how transitions between these functionally determined states occur. Similarly, crystal structures provide detailed information about different conformational states but are limited to static pictures; in addition, crystallography does not report the functional states corresponding to these static pictures or provide information on the dynamical transitions between states. Nuclear magnetic resonance (NMR) spectroscopy provides a powerful and complementary tool to these methods as it can probe conformational transitions both during gating and under experimental conditions that allow only specific functional states. Furthermore, NMR has an advantage over other techniques that can probe dynamics, such as fluorescence and electron paramagnetic resonance (EPR) spectroscopy, in that it does not require the use of mutants or additional bulky probes that can disrupt or otherwise fail to faithfully report the functionality and mobility of the native protein. Here, we investigated the conformational heterogeneity in specific functional states of the proton-gated, prokaryotic potassium channel KcsA incorporated into lipid bicelles, using solution state NMR combined with selective amino acid labeling.

The KcsA channel has been characterized both structurally and functionally and serves as a model potassium channel (Cuello et al., 1998; Doyle et al., 1998; Heginbotham et al., 1999; LeMasurier et al., 2001; Zhou et al., 2001). At neutral pH, KcsA is in the closed state, whereas at acidic pH the bundle crossing of the channel is open. Proton binding at the C-terminal intracellular bundle-crossing region, which contains a cluster of interacting ionizable residues, opens the channel by breaking the hydrogen bond network between these residues and increasing the local concentration of positive charges at high proton concentration, followed by slow inactivation at the selectivity filter (Doyle et al., 1998; Zhou et al., 2001; Cordero-Morales et al., 2006; Thompson et al., 2008; Cuello et al., 2010a). Several KcsA studies using NMR spectroscopy have contributed to our fundamental understanding of gating, pH sensing, and activation–inactivation coupling in KcsA and other po-

Correspondence to Crina M. Nimigean: crn2002@med.cornell.edu; or David Eliezer: dae2005@med.cornell.edu
I. Dikiy's present address is Structural Biology Initiative, Advanced Science Research Center, City University of New York, New York, NY 10031.

Abbreviations used: Cu-P, copper phenanthroline; DDM, dodecyl-maltopyranoside; DM, *n*-decyl maltoside; NMR, nuclear magnetic resonance.

The Rockefeller University Press $30.00
J. Gen. Physiol. 2016 Vol. 148 No. 2 119–132
www.jgp.org/cgi/doi/10.1085/jgp.201611602

Supplemental material can be found at:
http://doi.org/10.1085/jgp.201611602

tassium channels. NMR studies of KcsA in SDS micelles have provided residue assignments of both monomer and tetramer at several pH values (Chill et al., 2006, 2007). A pH sensor component of KcsA was identified by NMR experiments in dodecyl-maltopyranoside (DDM), based on the observation of pH-dependent chemical shifts for residue H25 (Takeuchi et al., 2007). Additional NMR studies focused on conformational changes occurring at the selectivity filter associated with inactivation gating (Ader et al., 2008, 2009; Bhate et al., 2010; Bhate and McDermott, 2012; Imai et al., 2012; Weingarth et al., 2014), in addition to coupling between the inactivation and activation gates (Baker et al., 2007; Ader et al., 2008, 2009; Wylie et al., 2014). NMR has proven to be a useful tool for assessing local dynamics at the selectivity filter and the activation gate of KcsA.

We sought to investigate the pH-dependent conformational changes of KcsA in the two states of the activation gate, open and closed, as well as the transition between these states, using NMR spectroscopy. We found that we were able to stabilize the functional closed state of the KcsA channel, even at low pH, by manipulating the lipid environment of the bicelles. Under these conditions, specifically labeled histidines at key positions in the channel report multiple conformational states in the closed channel. After addition of cardiolipin to the bicelles, which allows channel opening in functional experiments (Heginbotham et al., 1998; Valiyaveetil et al., 2002; Alvis et al., 2003; Marius et al., 2005), we also observed evidence for two conformational states represented by peaks distinct from those observed in the absence of cardiolipin. Analysis of the pH-dependent changes in the NMR spectra suggests that some of the observed closed states may represent preopen conformations or possibly asymmetric closed-channel configurations along the proton-dependent activation pathway.

MATERIALS AND METHODS

Protein expression, site-specific labeling, and purification

C-terminally His_6-tagged WT KcsA and most mutants were expressed from a pQE60 vector (QIAGEN) in either BL21 (DE3) T1-R (Sigma-Aldrich) or XL-1 Blue (Agilent Technologies) competent cells and grown in Luria broth (LB) with ampicillin. Cells were transformed with the appropriate vectors, and the resulting plates were scraped and pooled for inoculation the following day.

The site-specific labeling protocol was adapted from Marley et al. (2001). Cells were grown with aeration at 37°C until they reached an OD_{600} of ∼0.9 when they were spun at 5,000 rpm for 10 min at 4°C. The supernatant was removed and the cell pellet was washed with M9 salts (Sigma-Aldrich). Each cell pellet from 1 liter of media was then resuspended into 250 ml of minimal media (50 ml of 5× M9 salts, 100 µM $CaCl_2$, 1 mM $MgSO_4$, 0.25 g $AmCl_2$, 1 g dextrose, 2.5 ml of 100× BME vitamins (Sigma-Aldrich), and 100 µg/ml ampicillin) supplied with 20 mg [^{15}N]His or [^{13}C,^{15}N]His (uniformly labeled, Cambridge Isotope Laboratories). The remaining unlabeled amino acids were added in excess. The cells were recovered by aeration for 1 h at 37°C if induction occurred at 37°C or by aeration for 40 min at 37°C followed by 20 min of aeration at the intended induction temperature. After recovery, cells were induced by the addition of 0.5 mM IPTG. All KcsA mutants and WT were induced at 37°C for 4 h except for H25R (30°C, 4 h). After induction, cells were collected by centrifugation at 5,000 rpm for 10 min at 4°C. Cell pellets were stored on ice overnight at 4°C.

Purification of KcsA was adapted from Thompson et al. (2008), with minor modifications. Cell pellets were resuspended in buffer containing 50 mM Tris, pH 7.6, and 100 mM KCl and lysed by sonication. Membrane extraction occurred at room temperature for 2 h with 50 mM *n*-decyl maltoside (DM). Detergent-solubilized extract was separated by centrifugation for 45 min at 17,500 rpm at 4°C. Crude lysate was applied to a HiTrap chelating column charged with Ni^{+2} resin and washed with buffer B (100 mM KCl, 20 mM Tris, and 5 mM DM, pH 7.5) and 30 mM imidazole. Protein was eluted with buffer B and 300 mM imidazole and concentrated before incubation with chymotrypsin (enzyme to protein ratio was 1:50, by weight) for 2–3 h at room temperature. The proteolyzed protein was applied to a Sephadex-200 FPLC column equilibrated with buffer B, and protein eluting at the correct retention volume for KcsA ΔC was collected and pooled. Protein concentration was assayed by UV absorption spectroscopy at 280 nm and was calculated using an extinction coefficient of 33,570 $M^{-1}cm^{-1}$.

Reconstitution and bicelle formation

Incorporation of KcsA into POPC lipid bicelles was adapted from Morrison and Henzler-Wildman (2012). Long-chain lipid (POPC, cardiolipin; dried powder from Avanti Polar Lipids, Inc.) was used in a 100:1 molar ratio to the concentration of KcsA without exceeding 100 mM. Lipids were hydrated for several hours at room temperature at a concentration of 20 mg/ml in buffer containing 20 mM potassium phosphate, pH 7.0, and 20 mM NaCl. Lipids were sonicated for 1–2 min in a water bath before addition of 10% β-OG in buffer (50 µl per 20 mg long chain lipid) and incubated for 30 min at room temperature with gentle agitation. KcsA was then incubated with this mixture for 1 h at room temperature. Detergent was removed by incubation with 30 mg Bio-Beads (Bio-Rad Laboratories) per milligram of detergent at 4°C with three exchanges overnight. The resulting protein–lipid mixture was centrifuged at 40,000

rpm for 1 h at 4°C, and the pellet was resuspended into the final NMR buffer (20 mM potassium phosphate, pH 6.1, and 50 mM KCl) containing the short-chain lipid 06:0 PC (DHPC, Avanti Polar Lipids, Inc.) in a 3:1 ratio to long-chain lipid. The sample was then subjected to multiple freeze/thaw cycles to homogenize the bicelles. The sample typically contained 0.5–1 mM KcsA, and 10% by volume D_2O was added before NMR.

Cross-linking of L24C R117C

L24C/R117C KcsA (in WT and E71A backgrounds) was purified with the same method as WT, with minor modifications (Thompson et al., 2008). Cells were lysed and extracted in the presence of 1 mM TCEP, and 1 mM TCEP was also present in the Ni^{+2} affinity purification. The purified protein was applied to a Sephadex-200 column to remove TCEP. The eluted protein was concentrated and incubated with 2 mM copper phenanthroline (Cu-P) for 30 min at room temperature and then applied again to the Sephadex-200 column to remove Cu-P. After SDS-PAGE analysis to confirm cross-linking in the tetrameric form, the protein was chymotrypsinized, further purified over the Sephadex-200 column, and then reconstituted into bicelles as described for WT KcsA in the previous section. For electrophysiology, the protein was not chymotrypsinized and directly reconstituted into liposomes as described in the section below titled Reconstitution into liposomes and electrophysiology.

Crystallization and structure determination

Chymotrypsinized and cross-linked L24C/R117C KcsA was crystallized in complex with F_{ab} (Zhou et al., 2001) by sitting drop vapor diffusion method at 20°C. The reservoir solution contained polyethylene glycol (PEG) 400 (23–25% wt/vol), MES (100 mM, pH 6.25–6.75), and magnesium acetate (25 mM). Cryoprotection was achieved by a stepwise increase of the PEG concentration in the reservoir at a rate of 5% per day until a final concentration of 40% was reached. Crystals were frozen and stored in liquid nitrogen.

Diffraction data were collected at beamline 12-2 of the Stanford Synchrotron Radiation Light Source. Reflections were indexed, integrated, and scaled using XDS (Kabsch, 2010). The structure was solved by molecular replacement using Phaser (McCoy et al., 2007) and KcsA-Fab complex structure (PDB ID 1K4C) as search model (Zhou et al., 2001). The model was refined by iterative cycles of manual model building and refinement using COOT (Emsley and Cowtan, 2004) and Phenix (Adams et al., 2002), respectively. Structure validation was performed as described previously (Cheng et al., 2011) to exclude model bias.

Radioactive $^{86}Rb^+$ flux assay

$^{86}Rb^+$ flux assays were performed as previously described (Nimigean, 2006). In brief, liposomes were formed by reconstituting 0.5 µg E71A KcsA or E71A/L24C/R117C KcsA (solubilized in 5 mM DM) in 5 mg POPE/POPG (3:1) lipids (solubilized in 34 mM CHAPS) in buffer A (10 mM HEPES, 4 mM NMG, and 400 mM KCl, pH 7.0) and removing detergent over a G50 fine Sephadex column. Extra-liposomal K^+ was removed and buffer was exchanged to buffer B1 (10 mM HEPES, 4 mM NMG, and 400 mM sorbitol, pH 7.0) or B2 (10 mM HEPES, 4 mM NMG, and 400 mM sorbitol, pH 4.0) for assays performed at pH 7.0 or 4.0, respectively, over a G50 Sephadex column. Uptake was initiated by adding 600 µl buffer B1 or B2 containing $^{86}Rb^+$ (~1 µCi/ml) to 100 µl of liposomes. 100-µl aliquots were taken at the indicated time points, and the extra-liposomal $^{86}Rb^+$ was removed by passing them through 1.5-ml bed volume Dowex-NMG cation exchange columns. 1 µg/ml valinomycin was added at the end of each experiment to determine the maximum $^{86}Rb^+$ uptake. $^{86}Rb^+$ accumulated inside the liposomes in each sample was measured using liquid scintillation counter.

Reconstitution into liposomes and electrophysiology

L24C/R117C, H20A/H124R, and WT KcsA liposomes were formed using 3:1 POPE/POPG lipids (Avanti Polar Lipids, Inc.) as described previously (Thompson et al., 2008). For L24C/R117C, the resulting liposomes were split into two fractions, with one fraction being frozen and stored at −80°C in the presence of 1 mM TCEP and the other fraction frozen without TCEP. Liposomes were thawed on the day of use and sonicated briefly. Planar lipid bilayers (3:1 POPE/POPG, 7:3 DOPC/CL) were formed as previously described (Thompson et al., 2008). The trans chamber contained a solution with 10 mM succinate, pH 4.0, 35 mM KCl, and 15 mM KOH, and the cis chamber contained a solution with 10 mM HEPES, pH 7.0, 35 mM KCl, and 15 mM KOH for a total of 50 mM K^+ on each side. Changes in condition (pH, TCEP) were applied by perfusion of buffer into the trans chamber. In the case of L24C/R227C, liposomes that did not contain TCEP were painted onto the bilayer and channel incorporation was scouted at 100 mV (voltage reported as relative to the inside of the membrane, according to the electrophysiological convention, which in this system is the trans chamber). Incorporated channels were recorded at 100 mV, and an equivalent solution with 1 mM TCEP was perfused into the trans chamber. Channels were recorded at 100 mV for 30 min to ensure equilibration. For liposomes containing 1 mM TCEP, liposomes were painted onto the bilayer, and channel incorporation was scouted at 100 mV. Upon channel incorporation, the trans chamber solution was perfused to pH 7.0 to remove TCEP and close the channel, then perfused to pH 7.0 and 1 mM Cu-P to cross-link the closed channel, then to pH 4.0 and 1 mM Cu-P, then to pH 4.0 only to see if any channel openings were observed, and then finally back

to the original condition of pH 4.0 and 1 mM TCEP to rescue the original phenotype.

NMR data collection and analysis

[^{1}H,^{15}N]HSQC NMR experiments were performed on a 600-MHz Varian Inova (Agilent Technologies) and a 600-MHz Bruker Avance (Bruker Corporation) equipped with cryogenic probes. Typical experiments ran for 18 h and were the mean of 512 scans with 128 real and complex points. Typical spectral widths for [^{1}H,^{15}N]HSQC were 12 ppm in the ^{1}H dimension and 32 ppm in the ^{15}N dimension. All NMR experiments were conducted at 45°C. Protein concentrations were 500 µM to 1 mM, and lipid concentration was limited to 100 mM. NMR data were processed with NMRPipe (Delaglio et al., 1995) and analyzed with NMRViewJ (Johnson, 2004). Graphs were produced with Prism (GraphPad Software).

Mass spectrometry data collection and analysis

In brief, C-terminal labeling and quantitation to demonstrate relative abundance of KcsA cleavage sites was achieved using in-gel aniline labeling of protein C termini catalyzed by 1-ethyl-3-(3-dimethylaminopropyl) carbodiimide hydrochloride (EDC) for full-length and chymotrypsinized WT and mutant proteins. The most abundant C-terminal peptide from the cleaved proteins, after C-terminal aniline labeling (Panchaud et al., 2008) and in-gel chymotrypsin digestion, was W. FVG(G/R)EQERRGH|F. Full-length KcsA was processed to demonstrate "background" in-gel cleavage of H/F, where cleavage solely depends on in-gel enzyme activity. Aniline labeling is not complete, but it is assumed to be equivalent, independent of the C-terminal amino acid. Additional details and a table (Table S2) summarizing liquid chromatography mass spectrometry (LC-MS/MS) results are in the supplemental material.

Accession code

Protein Data Bank: Model and structure factors for the mutant KcsA structure L24C/R117C have been deposited under accession code 5E1A.

Online supplemental material

The supplemental materials and methods provide detailed information on mass spectrometry data collection and analysis. Fig. S1 shows the [^{1}H,^{15}N] HSQC spectrum for H25R compared with WT to show that H25 is not visible in PC bicelles. Fig. S2 is provided to illustrate the pH dependence of the chemical shifts of all the H124 resonances. Fig. S3 shows that all of the KcsA mutants investigated show similar pH dependences for the chemical shifts of all H124 peaks. Fig. S4 provides a zoomed-in view of the plot shown in Fig. 5 D, showing in detail the initial rates of radioactive flux uptake into liposomes loaded with the cross-linked–closed inactivation-free E71A/L24C/R117C KcsA construct for comparison with the inactivation-free E71A KcsA. Fig. S5 is provided to illustrate the characteristics of the current observed in the very rare occasions that channel activity appears when liposomes loaded with the cross-linked–closed L24C/R117C KcsA are fused into the lipid bilayer in the absence of reducing agents. Fig. S6 is provided to show that the [^{1}H,^{15}N]HSQC spectrum of the cross-linked–closed L24C/R117C KcsA displays identical pH dependence in chemical shifts to the WT spectrum. Fig. S7 shows the intensity ratios of H124 peak C1/C2 for WT KcsA in PC and PC:CL bicelles to illustrate the change in pH dependence between the two conformations in different lipid environments. Fig. S8 shows the [^{1}H,^{15}N]HNCA spectrum for [^{13}C,^{15}N]histidine-labeled WT KcsA in PC bicelles, comparing it with the [^{1}H,^{15}N]HSQC spectrum of [^{15}N]histidine-labeled WT KcsA in PC:CL bicelles. Table S1 is included to provide crystallographic data collection and refinement statistics for crystal structure determination of L24C/R117C KcsA. Table S2 is provided to summarize mass spectrometry experimental data for WT and L24C R117C KcsA. Online supplemental material is available at http://www.jgp.org/cgi/content/full/jgp.201611602/DC1.

RESULTS

KcsA H124 and H20 report multiple closed conformations as observed by NMR

We performed NMR experiments on a C-terminally truncated KcsA (residues 1–125, referred elsewhere as KcsA ΔC [Molina et al., 2004]), reconstituted into POPC/DHPC lipid bicelles (referred to as PC bicelles) to recapitulate the lipid environment of a cell membrane. The truncated KcsA channels are functional with pH dependence over the same pH range as full-length KcsA (Perozo et al., 1999; Cortes et al., 2001; Cuello et al., 2010a), and comparison of the NMR spectra of the two constructs shows that the overall structure is the same (Takeuchi et al., 2007; Imai et al., 2012). To study pH-dependent gating in KcsA by NMR, we specifically labeled the channel with [^{15}N]histidine to report both conformation and protonation states. We chose histidine because H25 is an important pH sensor of KcsA (Takeuchi et al., 2007; Thompson et al., 2008; Posson et al., 2013) and because labeled histidines do not result in metabolic scrambling like other labeled residues. Truncated KcsA contains three histidine residues. H25 is part of the pH sensor and is located at the intracellular end of first transmembrane helix (TM1) near the bundle crossing, or pH activation gate, H20 is located on the amphipathic helix at the N terminus, and H124 is located at the end of the second transmembrane helix (TM2) at the C terminus of the protein, located below the bundle crossing (Fig. 1).

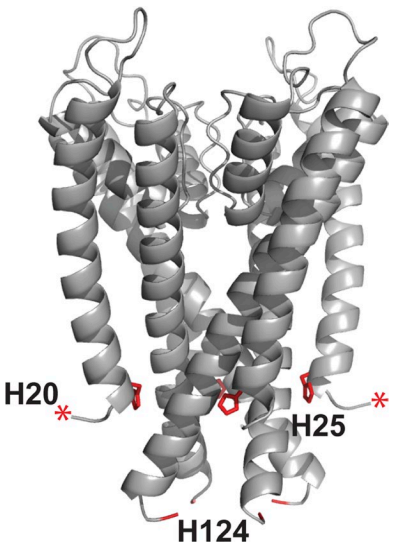

Figure 1. **Histidine residues in KcsA structure.** The KcsA crystal structure (PDB no. 1K4C) is shown highlighting the histidine residues labeled with ^{15}N in the NMR experiments. H20 (not observed in the structure and indicated by asterisks) lies on the N-terminal amphiphathic helix, H25 is the pH sensor and is located on TM1, and H124 resides on TM2 at the C-terminal end of the bundle crossing (side chains not modeled).

[^{1}H,^{15}N]HSQC experiments of WT KcsA ΔC were performed over a range of pHs between 3 and 8. Because solvent exchange effects led to the disappearance of peaks at higher pH, we show here spectra at lower pHs, which contain the highest number of peaks. At pH 4.5, the spectrum showed one very intense signal with a weaker nearby peak (Fig. 2 A). The channel was reported to be open at this pH in functional assays, but because of the lipid content of the bicelles (POPC), the channel is expected to be mostly closed at pH 4.5 in our conditions (Cuello et al., 1998; Iwamoto and Oiki, 2013). Bilayers composed primarily of PC are known to inhibit channel opening and largely limit KcsA to its closed state (Heginbotham et al., 1998; Valiyaveetil et al., 2002; Marius et al., 2005; Iwamoto and Oiki, 2013). Given the proximity of H124 to the C terminus of the KcsA ΔC construct, we provisionally assigned the most intense signal to H124. Equivalent spectra acquired using an H124R mutant indeed show that this signal disappears; in addition, the weaker signal nearby also disappears, suggesting that both of the signals originate from H124 and indicating that this residue can sample two distinct conformations in the closed state of the channel (Fig. 2 C). Further examination of the WT spectra at lower contour levels reveals additional peaks (Fig. 2 B), with several peaks within the typical chemical shift range of a histidine backbone NH group, and two shifted to lower proton and higher nitrogen chemical shift (down- and right-shifted). The peaks shifted down and right are also absent in the spectrum of the H124R mutant (Fig. 2 C), suggesting that they also originate from residue H124. Because C-terminal residues often exhibit backbone NMR NH resonances that are shifted down and right, we considered whether these two additional peaks might originate from proteins with H124 as the C-terminal residue. This possibility was supported by the fact that chymotrypsin, which was used to generate KcsA ΔC via cleavage after residue Phe 125, is not completely specific and can also cleave after His residues (Keil, 1992). Mass spectrometry analysis (see Materials and methods and supplemental text) confirmed the presence of a minor population of H124 truncated KcsA in our samples, corroborating the assignment of the weak shifted signals to these forms of the protein. Interestingly, the detection of two signals for H124 as the C-terminal residue further confirms that H124 samples two distinct conformations in the closed state.

To identify the remaining peaks, we collected [^{1}H,^{15}N] HSQC spectra with KcsA mutants H25R and H20A. The H25R spectrum (Fig. S1) looks equivalent to the WT ΔC spectrum, suggesting that we did not observe resonances originating from H25 in [^{1}H,^{15}N]HSQC experiments for the closed state. Mutation of H20 to an alanine results in the disappearance of the remaining unassigned peaks (Fig. 2 D), suggesting that these originate from residue H20 and indicating that this residue also samples multiple conformations that are in slow exchange in the closed state of the channel. This conformational heterogeneity suggests the existence of several stable states rather than elevated mobility caused by disorder. Based on chemical shift differences, the upper limit for this conformational exchange rate must be ∼5 Hz. This limit is similar to the rate of activation gating at the bundle crossing, whereas the rate of C-type inactivation occurs much slower, with time constants in the order of seconds (Cordero-Morales et al., 2006; Chakrapani et al., 2007).

Solution state NMR has been used to examine KcsA in several different detergent micelle contexts, including SDS, Fos-Choline, and DDM. Several of the resonances we observed in the presence of PC lipid bilayers correspond to previously observed signals in the context of micelles, including the primary resonances for H124 at pH 4.5 (observed at similar positions in SDS at pHs 4.2–8.0 [Chill et al., 2007] and Fos-Choline at pH 7.0 [Baker et al., 2007]) and one of the two C-terminal H124 resonances (observed for a construct ending at H124 in DDM micelles at pHs 4.1–5.0 [Takeuchi et al., 2007]). The case of H20 is more complicated because several signals seem to originate from this residue. Interestingly, upon elimination of His-124 via the H124R mutation, the remaining signals corresponding to H20 simplify into two major groups of resonances, one peak around 8.25/118 ppm (^{1}H/^{15}N) and one or two peaks around 8.5/118 ppm. These positions again resemble those previously observed in SDS and Fos-Choline at pH 4.0 (8.2/118 ppm [Baker et al., 2007; Chill et al.,

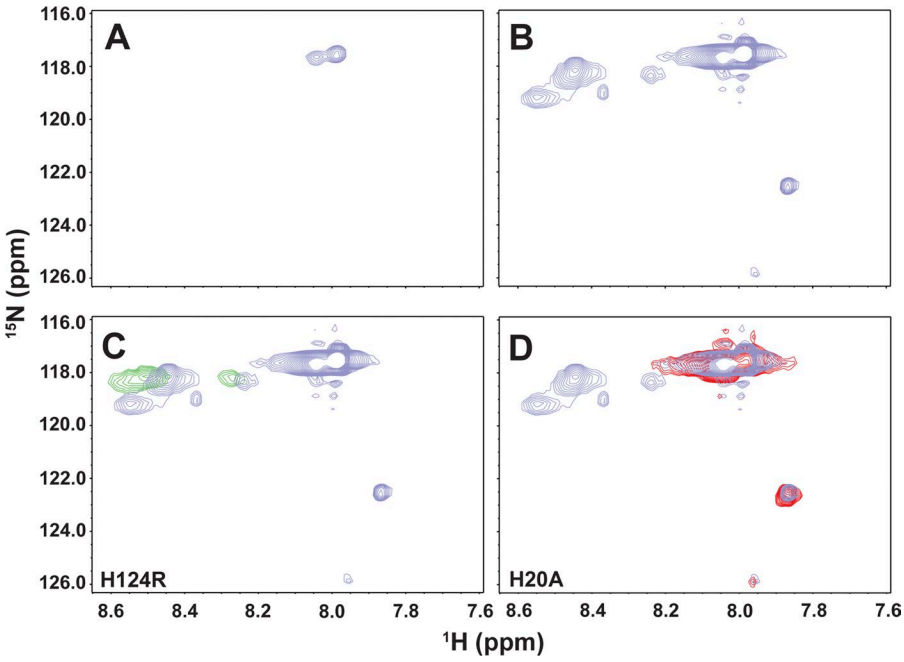

Figure 2. **Assignments of H124 and H20 peaks in the [^{1}H,^{15}N]HSQC spectrum of WT KcsA ΔC.** (A) The [^{15}N] HSQC NMR spectrum of [^{15}N]histidine-labeled WT KcsA ΔC at pH 4.5 shows two intense peaks. (B) Lowering the contour levels of the spectrum reveals multiple peaks of varying intensity in the range for backbone amides. Resonance assignments were achieved by collecting similar [^{1}H,^{15}N]HSQC on KcsA histidine mutants. (C) Superimposition of the HSQC spectrum of H124R KcsA ΔC (green) with the WT spectrum (purple) at pH 4.5, showing that four peaks correspond to H124. (D) Superimposition of the [^{15}N]HSQC spectrum of H20A KcsA ΔC (red) with the WT spectrum (purple) at pH 4.5, showing that four peaks correspond to H20.

2007]) and DDM at pHs 4.1–5.0 (8.6/120 ppm [Takeuchi et al., 2007]). It is not clear why a greater multiplicity of H20 signals is observed in the WT protein. Nevertheless, the fact that all but one of the signals observed in our spectra likely correspond to signals previously observed by others strongly supports the notion that the corresponding conformations of KcsA observed here represent stable well-defined conformational states.

Interestingly, previous NMR studies in detergent micelles only report one conformational state for residues H20 and H124, but different micelles capture different conformations (Baker et al., 2007; Chill et al., 2007; Takeuchi et al., 2007). SDS and Fos-Choline micelles capture one of our closed state conformations, whereas DDM at low pH appears to capture a different conformation. Our results indicate that the use of lipid bicelles allows for greater conformational heterogeneity in the protein, allowing it to sample a conformational ensemble that likely resembles its native physiological state more closely. We next inquired whether this conformational heterogeneity in the closed state is relevant for gating.

The multiple conformations of the closed state of KcsA are relevant to channel gating

Because KcsA is intrinsically sensitive to changes in pH, we investigated the behavior of the His resonances as a function of pH (Fig. 3). The C-terminal H124 peaks exhibit chemical shift changes as the protein is titrated (Fig. 3 A and Fig. S2). Of particular interest in our experiments, however, is the peak intensity and its dependence on pH, which can approximately reflect the relative population of a conformational state at a given pH. Interestingly, a comparison of the two C-terminal H124 peak intensities as a function of pH shows an anti-correlated relationship between pH 3.0 and 5 (Fig. 3 B). A similar anti-correlation is observed for the intensities of the primary H124 resonances (Fig. 3, C and D). This suggests that the two different conformations sampled by H124 in the closed state are capable of interconverting on a slow time scale and that pH influences which conformation is preferred by the protein, suggesting a role in gating. At pHs above 5, the NMR signal decreases, likely because of solvent exchange effects, and no longer reflects functional changes. H20 appears as multiple peaks at low pH (Figs. 2 and 3 E), with two peaks corresponding to previous studies (Baker et al., 2007; Chill et al., 2007; Takeuchi et al., 2007), but also with several additional peaks. There is no easily discernible relationship between the intensities of these three peaks as pH changes (Fig. 3 F), making it difficult to link these peaks to conformations represented by the H124 resonances. Nevertheless, the pH dependence of the balance of conformational states in the closed state of KcsA suggests that these fluctuations are physiologically relevant. We further tested this possibility by investigating several KcsA mutants with altered pH-gating behavior.

Previous electrophysiological studies have shown that mutation of two glutamates and a histidine (E118, E120, and H25) at the bundle crossing changes the pH dependence of KcsA (Thompson et al., 2008), leading to the proposal that E118 and H25 are the main pH-sensing residues in KcsA (Posson et al., 2013). We reasoned that if our NMR spectra correspond to multiple closed conformational states that are sampled during pH-dependent activation of KcsA (such as a preopen or intermediate closed state), some of our peaks may display altered chemical shift and/or inten-

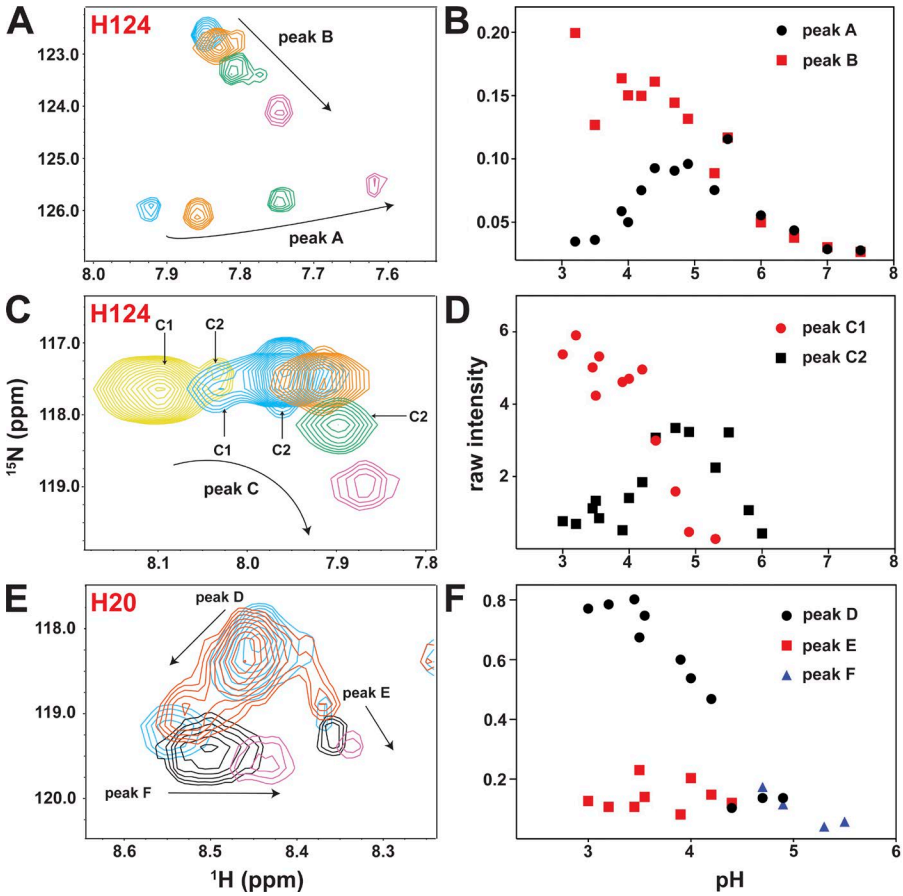

Figure 3. **Histidine peaks change with pH in the [^{1}H,^{15}N]HSQC spectrum of WT KcsA ΔC.** (A) pH-dependent chemical shift changes of the C-terminal H124 peaks (labeled peaks A and B) at pH 4.5 (blue), 5.5 (orange), 6.5 (green), and 7.5 (pink). Peaks A and B are observed through the pH range measured (pH 3–8). (B) Raw intensities plotted for C-terminal H124 peaks A and B as a function of pH. (C) pH-dependent chemical shift changes of the primary H124 peaks (labeled C1 and C2) at pH 3.0 (yellow), 4.5 (blue), 5.5 (orange), 6.5 (green), and 7.5 (pink). C1 and C2 peaks are marked with an arrow for pH 3.0 and 4.5. At pH 5.5, 6.5, and 7.5 only C2 is visible. (D) Raw intensities plotted for primary H124 peaks C1 and C2 as a function of pH. (E) pH-dependent chemical shift changes of the H20 peaks (labeled peaks D–F) at pH 3.7 (red), 4.0 (blue), 5.0 (black), and 5.5 (pink) showing their pH-dependent changes in chemical shift. (F) Raw intensities plotted for H20 peaks D–F.

sity in mutant channels that mimic protonation at pH sensor residues. To test this, we studied [^{15}N]His-labeled mutant channels E118A, E118A/E120A, and H25R and compared the NMR spectra to those of the WT. For all three mutants, the chemical shifts of the H20 and H124 signals and their pH dependence are similar to WT (Fig. S3), indicating that the mutant channels remain in a closed state ensemble. However, the intensity ratios of the two C-terminal H124 peaks display a lower (E118A, E118A/E120A) or absent (H25R) pH dependence compared with WT (Fig. 4). Because residue E118 is a weak pH sensor and residue H25 is a strong pH sensor (Posson et al., 2013), it stands to reason that E118A could result in a decrease in pH-dependent conformational exchange, whereas H25R could result in a loss of such pH-dependent conformational exchange. Therefore, mutation of pH-sensing residues did not eliminate any of these conformations but degraded the pH-dependent interconversion between the closed states, suggesting that these relate to channel activation by protons (Takeuchi et al., 2007; Posson et al., 2013).

We showed so far that H124 reports at least two slowly exchanging conformations that are dependent on pH, suggesting that these may be functional states related to channel gating. This is supported by the observation that the two conformations interchange over the pH range where the channel is known to increase its open probability in functional assays (pH 3–5 [Cuello et al., 1998; Heginbotham et al., 1999]) and that mutation of known pH sensors reduces this pH dependence.

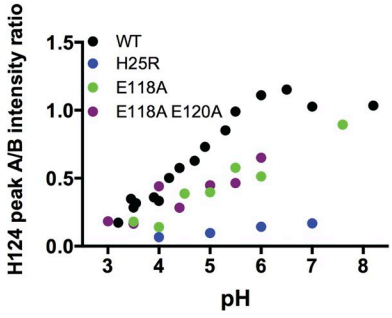

Figure 4. **pH sensor KcsA mutants alter the pH dependence of the H124 peak intensities.** Intensity ratios for C-terminal H124 peaks A/B (calculated from data shown in Fig. 3 B) are shown as a function of pH for WT, H25R, E118A, and E118A/E120A.

Cross-linking KcsA in a closed state limits the channel to one conformation

To further explore whether the multiple peaks we observed arise from different conformations visited by the channel in the closed state, we reduced the channel mobility by physically locking the channel using disulfide bonds in the closed conformation, as seen in the KcsA crystal structure (Fig. 1; Zhou et al., 2001). If the multiple peaks arise from channel mobility, we expect that the NMR spectrum of this channel would only display one peak for each histidine and that the peak intensity would be independent of pH. For this, we designed, expressed, and purified a channel where two residues at the KcsA bundle crossing, L24 on TM1 and R117 on TM2 (Fig. 5 A), were mutated to cysteines, which we chemically cross-linked using the oxidizing agent Cu-P. The intersubunit disulfide bonds then created a "belt" around the bundle crossing gate of the tetramer, preventing the helices from opening and thus trapping KcsA in the closed state. We confirmed that this construct is cross-linked and closed using SDS-PAGE analysis, $^{86}Rb^{+}$ flux assays, x-ray crystallography, and single-channel bilayer studies (Fig. 5, Figs. S4 and S5, and Table S1).

The [^{1}H,^{15}N]HSQC spectrum of cross-linked closed L24C/R117C KcsA ΔC in PC bicelles indeed shows the disappearance of multiple peaks when compared with the WT spectrum (Fig. 6). One of the two C-terminal H124 peaks disappears, as did one of the primary H124 resonances of the two closed conformations. The chemical shifts of the remaining H124 peaks were very similar to those observed in WT (Fig. S6). Additionally, the intensity of the remaining C-terminal H124 peak is greatly increased. This suggests that in the cross-linked channel, only one of the two closed conformations observed for the WT protein is populated. This is further supported by the observation that the pair of H124 peaks that remain visible in the cross-linked mutant, as well as the pair of peaks that disappear, exhibit similar intensity changes as a function of pH in the WT, suggesting that each pair originates from one conformation. The loss of resonances resulting from cross-linking KcsA into the closed state depicted by the KcsA crystal structure (Zhou et al., 2001) further supports that one set of peaks is representative of a functional conformational state adopted by KcsA during gating, as indicated by the behavior of the pH-gating mutants shown in the previous section.

Cross-linking also altered the population of the various H20 peaks. The peak at 8.2/118 ppm, corresponding to the resonances observed in SDS and Fos-Choline, disappears, whereas a single peak remained at ~8.5/119 ppm, reminiscent of the resonance observed in DDM. This is consistent with the scenario in which cross-linking the closed state of the channel traps a conformation similar to the one observed in DDM micelles.

Cardiolipin biases KcsA toward the open state and reveals H25

Using PC lipids allowed us to examine conformational heterogeneity within the closed channel without the complication of channel opening, which results in further, more dramatic conformational changes (Doyle et al., 1998; Zhou et al., 2001; Jiang et al., 2002; Cuello et al., 2010b,c). By using a different lipid bicelle composition that includes 15% cardiolipin, known to facilitate KcsA channel opening (Heginbotham et al., 1999; Valiyaveetil et al., 2002; Alvis et al., 2003; Marius et al., 2005), we could examine the open state of the channel with NMR. HSQC spectra of WT KcsA in bicelles containing 15% cardiolipin and 85% POPC (Fig. 7, referred to as PC:CL bicelles) at low pH show both similarities to and differences from spectra obtained in PC-only bicelles. The primary signals arising from H124 appear at the same position, but their intensities are altered. Notably, the H124 signal that disappears upon cross-linking (peak C2 in Fig. 3) becomes very intense in PC:CL bicelles, whereas the peak that remains in the cross-linked closed state (peak C1 in Fig. 3) becomes quite weak. The ratio of the two peaks also becomes insensitive to pH (Fig. S7). This suggests that although the conformations sampled by H124 are locally insensitive to the structural transitions that accompany channel opening (hence no chemical shift changes), the distribution of these conformations changes in different lipid compositions. In PC:CL, the signal reporting on a closed state conformation becomes very weak, whereas the signal that is eliminated by cross-linking, which may represent a preopen or intermediate closed state, becomes very intense. Interestingly, peaks corresponding to the H124 truncated KcsA do not appear (peaks A and B in Fig. 3), and only two H20 peaks are observed, at positions similar to those observed for the H124R mutant rather than the WT. Most interestingly, four novel peaks appear.

To explore the origin of these new peaks, we collected equivalent spectra using the H20A/H124R double mutant, which contains a sole remaining histidine, H25. This spectrum contains the four new signals, but not the H20 and H124 signals (Fig. 7 A, blue). Correspondingly, in the spectrum of the H25R mutant, the four new signals are absent while other signals were preserved. Thus, the new signals correspond to H25, indicating a new conformation present in PC:CL bicelles. HNCA spectra in PC:CL bicelles exhibit all four of these H25 peaks as well, confirming that they originate from a ^{13}C,^{15}N-labeled histidine (Fig. S8). One of the H25 signals, located at 8.3/120 ppm, corresponds well to a previous observation of an H25 resonance in DDM micelles at low pH (Takeuchi et al., 2007). A second signal at 8.7/121 ppm must correspond to an H25 backbone NH group in a different environment, indicating the presence of multiple conformations as we observed previously for the other histidines in the closed state (Fig. 2). The two ad-

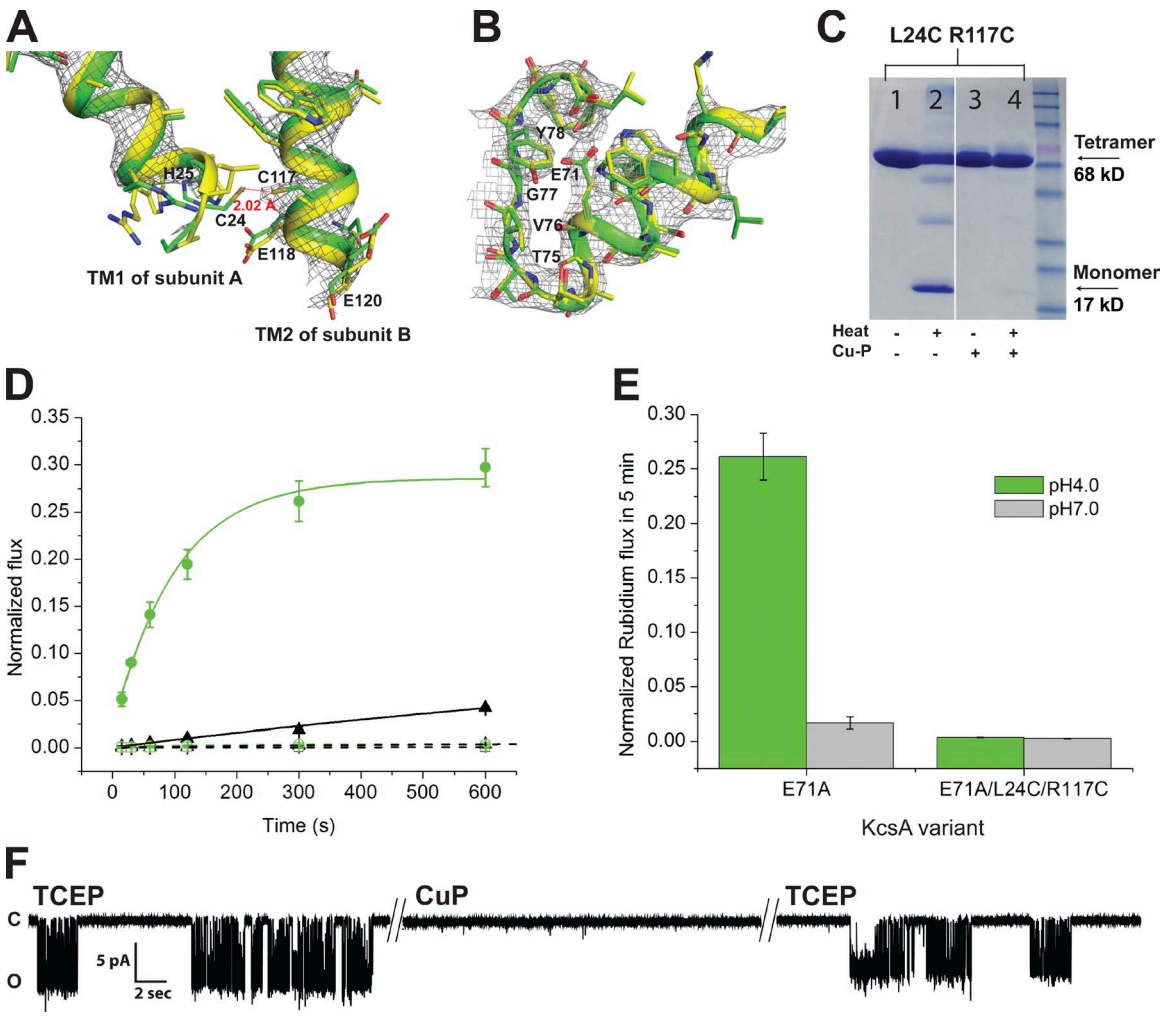

Figure 5. **L24C/R117C KcsA is cross-linked into the closed state and does not exhibit ion flux.** (A) The crystal structure of L24C/R117C KcsA was solved to 3.4 Å and was nearly identical to WT in the closed state. Comparison of L24C/R117C (green) and WT (yellow) models superimposed onto the electron density of the cross-linked mutant at the bundle-crossing region is shown. Several residues are shown, including the mutated cysteine residues C24 and C117. The two cysteine sulfur atoms are 2.02 Å apart in the structure, consistent with a disulfide bond. It is possible that the disulfide bond was lost in the structure because of radiation damage and therefore not visible in the electron density. (B) Comparison of L24C/R117C and WT at the selectivity filter, with key residues noted. (C) SDS-PAGE analysis of the cross-linked state of L24C/R117C KcsA in the absence of reducing agent. The channel is a tetramer in the absence of cross-linking agent Cu-P (lane 1), but when boiled for 10 min, half of the sample runs at the monomer size (lane 2), and bands at dimer, trimer, and tetramer size are also observed. After incubation with 2 mM Cu-P for 30 min at room temperature, the channel is cross-linked and runs at the tetramer size (lane 3), remaining stable even after boiling (lane 4). The white line indicates that intervening lanes have been spliced out. (D) $^{86}Rb^{+}$ uptake through E71A/L24C/R117C (cross-linked, see Materials and methods) at pH 4.0 (open green circles) and 7 (open black triangles) compared with that through E71A at pH 4.0 (closed green circles) and 7 (closed black triangles), at the same protein to lipid ratio reconstitutions. Protein-free liposomes showed no activity at either pH 7.0 (open black squares) or 4.0 (open green squares). Because flux through E71A at pH 4.0 is so large, we show a y-axis zoom in Fig. S3 to better evaluate the data. Symbols and error bars represent mean ± SE for experiments repeated in triplicate. (E) A bar graph summarizing the $^{86}Rb^{+}$ uptake from A. Normalized mean Rb^{+} uptake after 5 min is plotted for E71A and E71A/L24C/R117C at pH 4.0 and 7.0. The normalized Rb^{+} uptake at 300 s for E71A is 0.26 ± 0.02 at pH 4.0 and 0.019 ± 0.003 at pH 7, and for E71A/L24C/R117C the normalized uptake at 300 s is 0.0036 ± 3 × 10^{-4} at pH 4.0 and 0.0026 ± 2 × 10^{-4} at pH 7. Error bars represent SE for three experiments. (F) Representative trace from a single-channel electrophysiology experiment in planar lipid bilayers (3:1 POPE/POPG) with L24C/R117C liposomes reconstituted in the presence of 1 mM TCEP. Experiments were performed at 100 mV and filtered at 1 kHz. See Materials and methods for details.

ditional signals are shifted to higher ^{15}N and lower NH shifts, suggesting that they likely correspond to C-terminal resonances from a minor population of chymotryptic fragments with H25 at their C termini. The presence of such fragments was also confirmed by mass spectrometry, though it is presently unclear how such a small peptide would remain in the sample through detergent extraction, gel filtration, and exchange into bicelles.

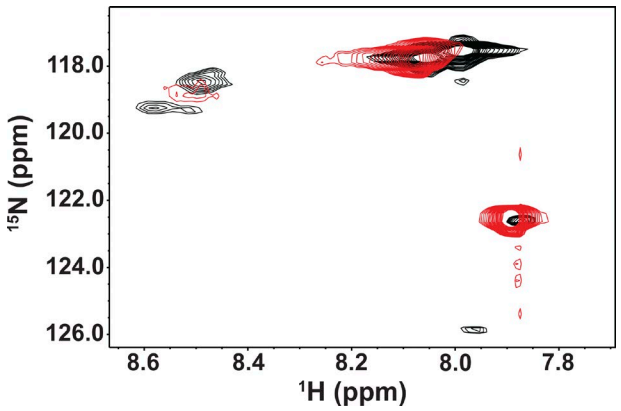

Figure 6. **L24C/R117C KcsA ΔC is cross-linked into the closed state.** [^{1}H,^{15}N]HSQC spectrum of L24C/R117C KcsA ΔC (red) superimposed onto the WT spectrum (black), both at pH 4.2, showing that H124 peaks A and C2 and two H20 peaks are missing in the spectrum of the cross-linked construct.

Because these H25 signals are observed only at pH 3–5 (no change in chemical shifts was observed in this pH range) and appear in the presence of cardiolipin, a lipid known to promote channel opening (Heginbotham et al., 1998; Valiyaveetil et al., 2002), we attribute them to open conformations of the channel. The open state likely leads to altered mobility for H25, making it observable in solution NMR spectra. This could result either from an increased degree of local mobility via release of hydrogen-bonding interactions at the bundle-crossing that hold the channel closed or possibly from a decrease in mobility/conformational exchange if H25 samples multiple conformations in the closed state and channel opening reduces this to fewer or a single conformation. In either case, our NMR data correlate with H25 appearing in conditions that promote the open state of the channel, supporting data that show higher KcsA activity in the presence of cardiolipin. The location of one H25 signal occurs near the expected random-coil chemical shifts for a backbone histidine residue, suggesting that in this conformation, H25 may not be involved in well-defined tertiary structure, as seen in the open state crystal structure of KcsA (Cuello et al., 2010c). The second H25 signal appears at a novel position not previously observed for this residue and is shifted well away from the random coil chemical shifts of a His residue; this suggests that in this conformation, H25 may be participating in tertiary structure interactions. The presence of two distinct H25 resonances suggests that, as in the case of the closed state, the open state of the channel also features multiple conformations.

Interestingly, peaks corresponding to H25 also appear in PC-only bicelles for the H20A/H124R double mutant at the same positions as in PC:CL bicelles, suggesting that this mutant channel is more open than WT (which does not show any peaks corresponding to H25 in PC-only bicelles). We investigated the new H20A/H124R double mutant electrophysiologically using single channel bilayer recordings, and indeed, this mutant was found to have a higher open probability than WT in POPE:POPG (3:1) planar lipid bilayers (Fig. 7 B).

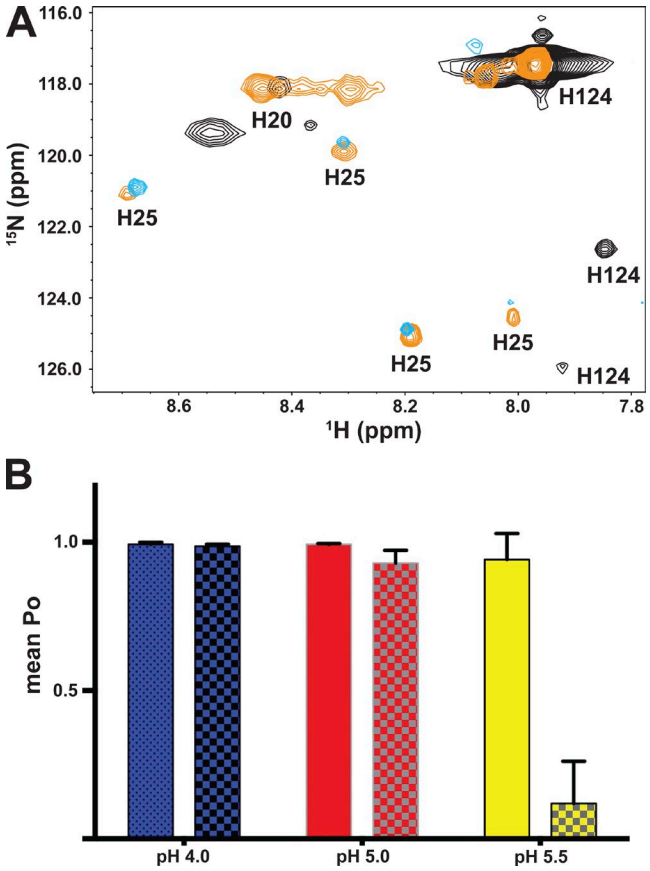

Figure 7. **Cardiolipin reveals open state of KcsA.** (A) [^{1}H,^{15}N]HSQC of KcsA in PC:CL bicelles. WT KcsA was reconstituted into PC:CL bicelles containing 15% cardiolipin. The [^{15}N]HSQC spectrum in PC:CL bicelles (orange) reveals similarities and differences compared with the [^{15}N]HSQC of KcsA in PC-only bicelles (black), both at pH 4.5. Additional peaks are observed in PC:CL conditions, identified as H25 by comparison with the [^{15}N]HSQC spectrum of the mutant H20A/H124R KcsA (blue) at pH 4.5, which retains H25 as its sole histidine. (B) KcsA mutant that allows visualization of H25 with NMR exhibits a higher open probability (Po) in planar lipid bilayers. Liposomes of H20A/H124R KcsA (in the background of a noninactivating E71A mutant commonly used for electrophysiology) were applied to 3:1 POPE:POPG planar lipid bilayers. Mean Po at 100 mV is shown for pH 4.0, 5.0, and pH 5.5, comparing E71A/H20A/H124R (solid bars) with E71A (checked bars [Posson et al., 2013]). The bars represent the mean ± SEs for $n = 3$ experiments.

DISCUSSION

Several crystal structures of KcsA and related potassium channels have provided a general picture of a subset of the conformational states that play a functional role in the process of gating. The closed state crystal structures

of KcsA (Doyle et al., 1998; Zhou et al., 2001) show a tight constriction at the bundle crossing, or activation gate. In contrast, the inner helices of the activation gate are widely splayed in the open state crystal structures of KcsA (Cuello et al., 2010c) and MthK (Jiang et al., 2002). We found here using solution NMR that there is considerable conformational heterogeneity within the open and closed states of KcsA, not visible in these crystal structures.

We observe multiple resonances for residues H20 and H124 in NMR spectra of WT KcsA ΔC in lipid bicelles composed of POPC, suggesting that at least two conformational states are in slow exchange on a millisecond–second timescale at any given pH. The elimination of a conformational state in the cross-linked channel suggests that the remaining state is the closed state, whereas the eliminated state may be an intermediate closed state or preopen state that is part of or separate from the gating pathway. Remarkably, inclusion of 15% cardiolipin into the POPC bicelles results in the appearance of new NMR resonances that were identified as the pH sensor residue H25, which is not observed in POPC-only bicelles. Similar to resonances observed in the closed state or states in POPC-only bicelles, H25 resonances in the open states appear at two different positions (the two upper resonances in the H25 quartet). This result implies that the open state ensemble of KcsA, like the closed state ensemble, encompasses more than a single stable conformation. At this point, it is possible only to speculate on the nature of these two conformations. One possible model describes the open state transitioning between two conformations. In one conformation, the N-terminal TM1 helix of KcsA interacts with the other helices of the channel, with H25 participating in tertiary interactions. In the second conformation, TM1 is detached from the other helices of the channel and H25 is not involved in tertiary structure. Clearly, determination of the pK_a of H25 in the closed and open states would be integral to understanding gating in KcsA. Unfortunately, we do not see H25 in the closed state and therefore cannot evaluate our previous proposal for a strongly perturbed pK_a in this state (Posson et al., 2013). The observation of H25 in PC:CL could in principle allow us to measure the pK_a of the pH sensor in the open state; however, these peaks only appear at low pH and do not move with pH, and therefore H25 is likely not titrating in this regime.

These results suggest we have a strong correlation between our NMR and electrophysiology data, linking structural features to functional properties of the channel. Although there are certainly differences between lipid bilayer and lipid bicelles in terms of curvature, fluidity, pressure, and thickness (Lundbæk et al., 1996; Cross et al., 2011; Warschawski et al., 2011), our data support that at least in KcsA, the functional attributes of the channel are consistent between the two lipid environments. The cross-linked closed channel and channels in POPC are shown to have a lower open probability in electrophysiology studies and also appear to be in the closed state in NMR studies. Conversely, mutants showing modified pH dependence in electrophysiological studies (H25R, E118A, E118A/E120A, H20A/H124R) also display an altered pH dependence or change in NMR spectra compared with WT in POPC; the pH dependence of the peaks in these spectra as well as the fact that channels in PC:CL bicelles produce alternate spectra suggest that we also observe the open state of KcsA. The pH dependence of slowly exchanging conformations in the closed state and the appearance of H25 in conditions supporting the open state suggest that the conformations we observe play a functional role in gating. The slow exchange occurs on the timescale that could be consistent with activation gating, providing further support that the conformational exchange we observe may be functional.

It is also interesting to note that the resonances observed for H20 in the presence of cardiolipin are located in positions similar to those observed for the closed state of the H124R mutant in the absence of cardiolipin and different from those observed for the closed state of the WT protein. This suggests the possibility that in the presence of PC lipids, the regions containing H124 and H20 might interact. H20 is located in a membrane surface–bound helix that is generally not directly visualized in structures of KcsA (Doyle et al., 1998; Zhou et al., 2001; Cuello et al., 2010c), and thus its position relative to H124 is not known. Fewer H20 peaks are observed in the presence of CL, suggesting the interaction between the two regions may be eliminated in the open state. Furthermore, when we examined the H20A/H124R double mutant in POPC-only bicelles to identify H25 resonances in the PC:CL spectrum, we observed all four H25 resonances. This result predicts that the H20A/H124R mutant populates the open state even in POPC-only bicelles, indicating increased open probability as demonstrated by electrophysiology experiments. If this were in fact the case, it would suggest that interactions between the C terminus of TM2 and the H20-containing helix might be important in stabilizing the closed conformation of the channel.

The notion of multiple closed states in the gating path of ion channels was initially proposed many years ago (Hodgkin and Huxley, 1952; Armstrong, 1969) and is supported by decades of ion channel electrophysiology (Magleby, 2003) and, more recently, for KcsA by fluorescence (Blunck et al., 2008), computational (Zhong and Guo, 2009; Linder et al., 2013), and electrophysiology (Thompson et al., 2008) studies suggesting that opening of the four subunits of KcsA does not occur in a concerted fashion but in a stepwise, cooperative manner that includes multiple closed states

(Blunck et al., 2008). Asymmetric opening of the channel is further supported by a computational study that observed that the channel remains closed upon opening of one or two subunits, but that opening of three subunits is required to open the channel (Linder et al., 2013). It has also been suggested that the four subunits move in an asymmetric fashion before opening, and that multiple states are sampled until an optimal conformation is achieved for opening (Zhong and Guo, 2009). The observation of subconductances in an electrophysiological study also supports the notion of asymmetric subunit movements in KcsA (Thompson et al., 2008). The novel intermediate closed state we observe in our NMR study could reflect this asymmetry in channel opening. Assignation of closed states to structurally different conformations is usually complicated by the fact that they cannot be easily observed in existing experimental assays (because closed states do not allow ion fluxes). Similar asymmetries could also exist in the open state ensemble of the channel. Several other studies suggest local dynamical changes contribute to multiple closed states that play a functional role in gating (Zhong and Guo, 2009; Hulse et al., 2014; Raghuraman et al., 2014). Our study, which presents novel closed and open conformations of KcsA, further supports this hypothesis, and additional studies of dynamics in the closed state will aid in the fundamental understanding of gating in potassium channels.

Conclusions

In this study, we used NMR spectroscopy to elucidate different conformational states that are populated by KcsA in the closed and open states. Conformational dynamics in proteins is increasingly found experimentally to be important for their function. We observe that in particular functional states of KcsA, there are significant conformational fluctuations on a slow time scale that are demonstrated to be important for gating. Using NMR, we were able to capture conformational heterogeneity of KcsA in both its closed and open states, showing that an equilibrium between multiple conformations within specific functional states is critical for channel activation in KcsA. To our knowledge, this is the first direct structural measurement on a molecular scale of multiple closed and open states in KcsA that are shown to be relevant to gating.

ACKNOWLEDGMENTS

We would like to thank C. Bracken for assistance with NMR, as well as A. McDermott for helpful discussions. We thank A. Thompson for providing electrophysiology data for KcsA WT. We also acknowledge B. Dill at The Rockefeller University for mass spectrometry data collection and interpretation. V. Stojanoff provided assistance at the Stanford Synchrotron Radiation Lightsource beamlines 14-1 and 12.2, which is supported by the U.S. Department of Energy (DOE) under contract no. DE-AC02-76SF00515, the DOE Office of Biological and Environmental Research, and by the National Institutes of Health, National Institute of General Medical Sciences (including P41GM103393).

D. Eliezer and C.M. Nimigean are members of the New York Structural Biology Center (NYSBC). The data collected at NYSBC was made possible by a grant from the New York State Foundation for Science, Technology, and Innovation (NYSTAR). This work was supported by National Institutes of Health grants RO1GM088352 and RO1GM088352-S1 (to C.M. Nimigean) and R37AG019391 (D. Eliezer).

The authors declare no competing financial interests.

Merritt Maduke served as editor.

Submitted: 4 April 2016
Accepted: 27 June 2016

REFERENCES

Adams, P.D., R.W. Grosse-Kunstleve, L.W. Hung, T.R. Ioerger, A.J. McCoy, N.W. Moriarty, R.J. Read, J.C. Sacchettini, N.K. Sauter, and T.C. Terwilliger. 2002. PHENIX: building new software for automated crystallographic structure determination. *Acta Crystallogr. D Biol. Crystallogr.* 58:1948–1954. http://dx.doi.org/10.1107/S0907444902016657

Ader, C., R. Schneider, S. Hornig, P. Velisetty, E.M. Wilson, A. Lange, K. Giller, I. Ohmert, M.F. Martin-Eauclaire, D. Trauner, et al. 2008. A structural link between inactivation and block of a K^+ channel. *Nat. Struct. Mol. Biol.* 15:605–612. http://dx.doi.org/10.1038/nsmb.1430

Ader, C., R. Schneider, S. Hornig, P. Velisetty, V. Vardanyan, K. Giller, I. Ohmert, S. Becker, O. Pongs, and M. Baldus. 2009. Coupling of activation and inactivation gate in a K^+-channel: potassium and ligand sensitivity. *EMBO J.* 28:2825–2834. http://dx.doi.org/10.1038/emboj.2009.218

Alvis, S.J., I.M. Williamson, J.M. East, and A.G. Lee. 2003. Interactions of anionic phospholipids and phosphatidylethanolamine with the potassium channel KcsA. *Biophys. J.* 85:3828–3838. http://dx.doi.org/10.1016/S0006-3495(03)74797-3

Armstrong, C.M. 1969. Inactivation of the potassium conductance and related phenomena caused by quaternary ammonium ion injection in squid axons. *J. Gen. Physiol.* 54:553–575. http://dx.doi.org/10.1085/jgp.54.5.553

Baker, K.A., C. Tzitzilonis, W. Kwiatkowski, S. Choe, and R. Riek. 2007. Conformational dynamics of the KcsA potassium channel governs gating properties. *Nat. Struct. Mol. Biol.* 14:1089–1095. http://dx.doi.org/10.1038/nsmb1311

Bhate, M.P., and A.E. McDermott. 2012. Protonation state of E71 in KcsA and its role for channel collapse and inactivation. *Proc. Natl. Acad. Sci. USA.* 109:15265–15270. http://dx.doi.org/10.1073/pnas.1211900109

Bhate, M.P., B.J. Wylie, L. Tian, and A.E. McDermott. 2010. Conformational dynamics in the selectivity filter of KcsA in response to potassium ion concentration. *J. Mol. Biol.* 401:155–166. http://dx.doi.org/10.1016/j.jmb.2010.06.031

Blunck, R., H. McGuire, H.C. Hyde, and F. Bezanilla. 2008. Fluorescence detection of the movement of single KcsA subunits reveals cooperativity. *Proc. Natl. Acad. Sci. USA.* 105:20263–20268. http://dx.doi.org/10.1073/pnas.0807056106

Chakrapani, S., J.F. Cordero-Morales, and E. Perozo. 2007. A quantitative description of KcsA gating I: macroscopic currents. *J. Gen. Physiol.* 130:465–478. http://dx.doi.org/10.1085/jgp.200709843

Cheng, W.W., J.G. McCoy, A.N. Thompson, C.G. Nichols, and C.M. Nimigean. 2011. Mechanism for selectivity-inactivation coupling in KcsA potassium channels. *Proc. Natl. Acad. Sci. USA.* 108:5272–5277. http://dx.doi.org/10.1073/pnas.1014186108

Chill, J.H., J.M. Louis, C. Miller, and A. Bax. 2006. NMR study of the tetrameric KcsA potassium channel in detergent micelles. *Protein Sci.* 15:684–698. http://dx.doi.org/10.1110/ps.051954706

Chill, J.H., J.M. Louis, F. Delaglio, and A. Bax. 2007. Local and global structure of the monomeric subunit of the potassium channel KcsA probed by NMR. *Biochim. Biophys. Acta.* 1768:3260–3270. http://dx.doi.org/10.1016/j.bbamem.2007.08.006

Cordero-Morales, J.F., L.G. Cuello, Y. Zhao, V. Jogini, D.M. Cortes, B. Roux, and E. Perozo. 2006. Molecular determinants of gating at the potassium-channel selectivity filter. *Nat. Struct. Mol. Biol.* 13:311–318. http://dx.doi.org/10.1038/nsmb1069

Cortes, D.M., L.G. Cuello, and E. Perozo. 2001. Molecular architecture of full-length KcsA: role of cytoplasmic domains in ion permeation and activation gating. *J. Gen. Physiol.* 117:165–180. http://dx.doi.org/10.1085/jgp.117.2.165

Cross, T.A., M. Sharma, M. Yi, and H.X. Zhou. 2011. Influence of solubilizing environments on membrane protein structures. *Trends Biochem. Sci.* 36:117–125. http://dx.doi.org/10.1016/j.tibs.2010.07.005

Cuello, L.G., J.G. Romero, D.M. Cortes, and E. Perozo. 1998. pH-dependent gating in the *Streptomyces lividans* K^+ channel. *Biochemistry.* 37:3229–3236. http://dx.doi.org/10.1021/bi972997x

Cuello, L.G., D.M. Cortes, V. Jogini, A. Sompornpisut, and E. Perozo. 2010a. A molecular mechanism for proton-dependent gating in KcsA. *FEBS Lett.* 584:1126–1132. http://dx.doi.org/10.1016/j.febslet.2010.02.003

Cuello, L.G., V. Jogini, D.M. Cortes, and E. Perozo. 2010b. Structural mechanism of C-type inactivation in K^+ channels. *Nature.* 466:203–208. http://dx.doi.org/10.1038/nature09153

Cuello, L.G., V. Jogini, D.M. Cortes, A. Sompornpisut, M.D. Purdy, M.C. Wiener, and E. Perozo. 2010c. Design and characterization of a constitutively open KcsA. *FEBS Lett.* 584:1133–1138. http://dx.doi.org/10.1016/j.febslet.2010.02.015

Delaglio, F., S. Grzesiek, G.W. Vuister, G. Zhu, J. Pfeifer, and A. Bax. 1995. NMRPipe: a multidimensional spectral processing system based on UNIX pipes. *J. Biomol. NMR.* 6:277–293. http://dx.doi.org/10.1007/BF00197809

Doyle, D.A., J. Morais Cabral, R.A. Pfuetzner, A. Kuo, J.M. Gulbis, S.L. Cohen, B.T. Chait, and R. MacKinnon. 1998. The structure of the potassium channel: molecular basis of K^+ conduction and selectivity. *Science.* 280:69–77. http://dx.doi.org/10.1126/science.280.5360.69

Emsley, P., and K. Cowtan. 2004. Coot: model-building tools for molecular graphics. *Acta Crystallogr. D Biol. Crystallogr.* 60:2126–2132. http://dx.doi.org/10.1107/S0907444904019158

Heginbotham, L., L. Kolmakova-Partensky, and C. Miller. 1998. Functional reconstitution of a prokaryotic K^+ channel. *J. Gen. Physiol.* 111:741–749. http://dx.doi.org/10.1085/jgp.111.6.741

Heginbotham, L., M. LeMasurier, L. Kolmakova-Partensky, and C. Miller. 1999. Single *Streptomyces lividans* K^+ channels: functional asymmetries and sidedness of proton activation. *J. Gen. Physiol.* 114:551–560. http://dx.doi.org/10.1085/jgp.114.4.551

Hodgkin, A.L., and A.F. Huxley. 1952. A quantitative description of membrane current and its application to conduction and excitation in nerve. *J. Physiol.* 117:500–544. http://dx.doi.org/10.1113/jphysiol.1952.sp004764

Hulse, R.E., J.R. Sachleben, P.C. Wen, M. Moradi, E. Tajkhorshid, and E. Perozo. 2014. Conformational dynamics at the inner gate of KcsA during activation. *Biochemistry.* 53:2557–2559. http://dx.doi.org/10.1021/bi500168u

Imai, S., M. Osawa, K. Mita, S. Toyonaga, A. Machiyama, T. Ueda, K. Takeuchi, S. Oiki, and I. Shimada. 2012. Functional equilibrium of the KcsA structure revealed by NMR. *J. Biol. Chem.* 287:39634–39641. http://dx.doi.org/10.1074/jbc.M112.401265

Iwamoto, M., and S. Oiki. 2013. Amphipathic antenna of an inward rectifier K^+ channel responds to changes in the inner membrane leaflet. *Proc. Natl. Acad. Sci. USA.* 110:749–754. http://dx.doi.org/10.1073/pnas.1217323110

Jiang, Y., A. Lee, J. Chen, M. Cadene, B.T. Chait, and R. MacKinnon. 2002. Crystal structure and mechanism of a calcium-gated potassium channel. *Nature.* 417:515–522. http://dx.doi.org/10.1038/417515a

Johnson, B.A. 2004. Using NMRView to visualize and analyze the NMR spectra of macromolecules. *Methods Mol. Biol.* 278:313–352.

Kabsch, W. 2010. Xds. *Acta Crystallogr. D Biol. Crystallogr.* 66:125–132. http://dx.doi.org/10.1107/S0907444909047337

Keil, B. 1992. Specificity of Proteolysis. Springer-Verlag, New York. 336 pp. http://dx.doi.org/10.1007/978-3-642-48380-6

LeMasurier, M., L. Heginbotham, and C. Miller. 2001. KcsA: It's a potassium channel. *J. Gen. Physiol.* 118:303–314. http://dx.doi.org/10.1085/jgp.118.3.303

Linder, T., B.L. de Groot, and A. Stary-Weinzinger. 2013. Probing the energy landscape of activation gating of the bacterial potassium channel KcsA. *PLOS Comput. Biol.* 9:e1003058. http://dx.doi.org/10.1371/journal.pcbi.1003058

Lundbæk, J.A., P. Birn, J. Girshman, A.J. Hansen, and O.S. Andersen. 1996. Membrane stiffness and channel function. *Biochemistry.* 35:3825–3830. http://dx.doi.org/10.1021/bi952250b

Magleby, K.L. 2003. Gating mechanism of BK (Slo1) channels: so near, yet so far. *J. Gen. Physiol.* 121:81–96. (published erratum appears in *J. Gen. Physiol.* 2004. 123:469) http://dx.doi.org/10.1085/jgp.20028721

Marius, P., S.J. Alvis, J.M. East, and A.G. Lee. 2005. The interfacial lipid binding site on the potassium channel KcsA is specific for anionic phospholipids. *Biophys. J.* 89:4081–4089. http://dx.doi.org/10.1529/biophysj.105.070755

Marley, J., M. Lu, and C. Bracken. 2001. A method for efficient isotopic labeling of recombinant proteins. *J. Biomol. NMR.* 20:71–75. http://dx.doi.org/10.1023/A:1011254402785

McCoy, A.J., R.W. Grosse-Kunstleve, P.D. Adams, M.D. Winn, L.C. Storoni, and R.J. Read. 2007. Phaser crystallographic software. *J. Appl. Cryst.* 40:658–674. http://dx.doi.org/10.1107/S0021889807021206

Molina, M.L., J.A. Encinar, F.N. Barrera, G. Fernández-Ballester, G. Riquelme, and J.M. González-Ros. 2004. Influence of C-terminal protein domains and protein-lipid interactions on tetramerization and stability of the potassium channel KcsA. *Biochemistry.* 43:14924–14931. http://dx.doi.org/10.1021/bi048889+

Morrison, E.A., and K.A. Henzler-Wildman. 2012. Reconstitution of integral membrane proteins into isotropic bicelles with improved sample stability and expanded lipid composition profile. *Biochim. Biophys. Acta.* 1818:814–820. http://dx.doi.org/10.1016/j.bbamem.2011.12.020

Nimigean, C.M. 2006. A radioactive uptake assay to measure ion transport across ion channel-containing liposomes. *Nat. Protoc.* 1:1207–1212. http://dx.doi.org/10.1038/nprot.2006.166

Panchaud, A., J. Hansson, M. Affolter, R. Bel Rhlid, S. Piu, P. Moreillon, and M. Kussmann. 2008. ANIBAL, stable isotope-based quantitative proteomics by aniline and benzoic acid labeling of amino and carboxylic groups. *Mol. Cell. Proteomics.* 7:800–812. http://dx.doi.org/10.1074/mcp.M700216-MCP200

Perozo, E., D.M. Cortes, and L.G. Cuello. 1999. Structural rearrangements underlying K^+-channel activation gating. *Science.* 285:73–78. http://dx.doi.org/10.1126/science.285.5424.73

Posson, D.J., A.N. Thompson, J.G. McCoy, and C.M. Nimigean. 2013. Molecular interactions involved in proton-dependent gating in KcsA potassium channels. *J. Gen. Physiol.* 142:613–624. http://dx.doi.org/10.1085/jgp.201311057

Raghuraman, H., S.M. Islam, S. Mukherjee, B. Roux, and E. Perozo. 2014. Dynamics transitions at the outer vestibule of the KcsA potassium channel during gating. *Proc. Natl. Acad. Sci. USA.* 111:1831–1836. (published erratum appears in *Proc. Natl. Acad. Sci. USA.* 2014. 111:4644) http://dx.doi.org/10.1073/pnas.1314875111

Takeuchi, K., H. Takahashi, S. Kawano, and I. Shimada. 2007. Identification and characterization of the slowly exchanging pH-dependent conformational rearrangement in KcsA. *J. Biol. Chem.* 282:15179–15186. http://dx.doi.org/10.1074/jbc.M608264200

Thompson, A.N., D.J. Posson, P.V. Parsa, and C.M. Nimigean. 2008. Molecular mechanism of pH sensing in KcsA potassium channels. *Proc. Natl. Acad. Sci. USA.* 105:6900–6905. http://dx.doi.org/10.1073/pnas.0800873105

Valiyaveetil, F.I., Y. Zhou, and R. MacKinnon. 2002. Lipids in the structure, folding, and function of the KcsA K^+ channel. *Biochemistry.* 41:10771–10777. http://dx.doi.org/10.1021/bi026215y

Warschawski, D.E., A.A. Arnold, M. Beaugrand, A. Gravel, É. Chartrand, and I. Marcotte. 2011. Choosing membrane mimetics for NMR structural studies of transmembrane proteins. *Biochim. Biophys. Acta.* 1808:1957–1974. http://dx.doi.org/10.1016/j.bbamem.2011.03.016

Weingarth, M., E.A. van der Cruijsen, J. Ostmeyer, S. Lievestro, B. Roux, and M. Baldus. 2014. Quantitative analysis of the water occupancy around the selectivity filter of a K^+ channel in different gating modes. *J. Am. Chem. Soc.* 136:2000–2007. http://dx.doi.org/10.1021/ja411450y

Wylie, B.J., M.P. Bhate, and A.E. McDermott. 2014. Transmembrane allosteric coupling of the gates in a potassium channel. *Proc. Natl. Acad. Sci. USA.* 111:185–190. http://dx.doi.org/10.1073/pnas.1319577110

Zhong, W., and W. Guo. 2009. Mixed modes in opening of KcsA potassium channel from a targeted molecular dynamics simulation. *Biochem. Biophys. Res. Commun.* 388:86–90. http://dx.doi.org/10.1016/j.bbrc.2009.07.123

Zhou, Y., J.H. Morais-Cabral, A. Kaufman, and R. MacKinnon. 2001. Chemistry of ion coordination and hydration revealed by a K^+ channel-Fab complex at 2.0 Å resolution. *Nature.* 414:43–48. http://dx.doi.org/10.1038/35102009

SUPPLEMENTAL MATERIAL

Kim et al., http://www.jgp.org/cgi/content/full/jgp.201611602/DC1

Mass spectrometry data collection and analysis

LC-MS/MS identification of cleavage sites

To demarcate the C-terminal boundary after incubation with chymotrypsin, cleaved proteins were analyzed by bottom-up LC-MS/MS. Cleaved proteins were separated by SDS-PAGE, excised, and treated as follows.

Sample preparation for fragment ending in H124/F125

Although proteolysis of KcsA was achieved using chymotrypsin, the sequence requirements of the C terminus made it necessary to use chymotrypsin rather than other available enzymes to generate detectable peptides for MS analysis. Thus, aniline labeling (Panchaud et al., 2008), which reacts with carboxyl groups, marking the protein C terminus (and also aspartic acid and glutamic acid residues), was used to provide evidence for C-terminal position before proteolytic cleavage during MS sample prep. Chymotrypsinized KcsA samples were either labeled by aniline or left unlabeled and proteolytically digested. In brief, 100 mM aniline was incubated with gel bands in 200 mM pyridine, pH 5, with 200 mM EDC at room temperature for 2 h. After labeling, bands were extensively washed with 100 mM ammonium bicarbonate and acetonitrile, increasing the organic concentration in each washing step. Proteins were reduced in 10 mM dithiothreitol (Sigma-Aldrich) before alkylation of cysteines with iodoacetamide (Sigma-Aldrich). After dehydrating gel bands, a solution of 20 ng/µl chymotrypsin (Promega) in 100 mM ammonium bicarbonate was absorbed into the band for overnight digestion.

Sample preparation for fragment ending in H25

To generate ideal proteolytic peptides for samples containing H25 at the C terminus, gel bands were digested with either 20 ng/µl trypsin (Promega) or LysC (Wako Pure Chemical Industries) after cysteine alkylation.

LC-MS/MS analysis

Each sample was analyzed by nano LC-MS/MS (Dionex 3000 HPLC coupled to Q-Exactive mass spectrometer; Thermo Fisher Scientific). Peptides were separated at 200 nl/min using a "typical" gradient for unlabeled peptides or gradient to a higher percentage organic to elute the hydrophobic aniline-labeled peptides: (a) a gradient increasing from 5% B to 30% B in 75 minutes (A: 0.1% formic acid, B: acetonitrile/0.1% formic acid) or (b) a gradient increasing from 5% B to 60% B in 75 min. Peptides were loaded onto a trap column before separation on a packed-in-emitter C_{18} column (75 µm by 12 cm, 3 µm particles; Nikkyo Technos Co., Ltd.). For data-dependent analysis of peptide/modification identification, the mass spectrometer was operated in "preferred mode": fragmentation of up to 20 ions per cycle using an under fill ratio of 1%. MS spectra (m/z range: 300–1,400) were recorded at a resolution of 70,000 (AGC: 5e5) and MS/MS spectra at 17,500 (AGC: 2e5) with a lowest m/z of 100. Generated LC-MS/MS data were queried against a custom database (containing contaminants, irrelevant entries, and the proteins of interest) using Mascot, with carbamidomethylation of cysteine (C) as a static modification and the following variable modifications as appropriate: oxidation of methionine, acetylation of protein N termini, aniline labeling on D, E, and C terminus, and semi-specific enzyme restrictions with trypsin, LysC, or chymotrypsin. Mass accuracy requirements were 10 ppm for MS and 20 mmu for MS/MS. Data are summarized in Table S2.

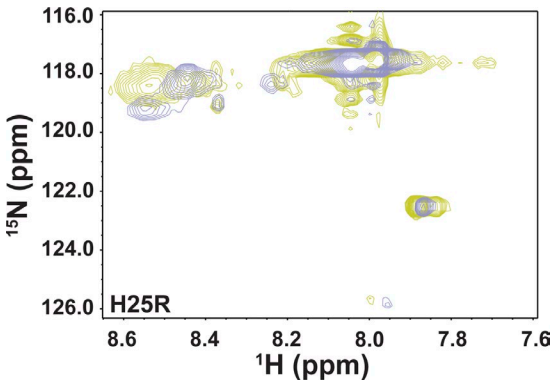

Figure S1. **[^{1}H,^{15}N]HSQC spectrum of H25R KcsA.** The [^{1}H,^{15}N]HSQC spectrum of H25R KcsA at pH 4.0 (lime) is compared with the [^{15}N]HSQC spectrum of WT KcsA at pH 4.2 (lavender). The contours of the H25R spectrum are set to low to observe the H124 peak A and B signals.

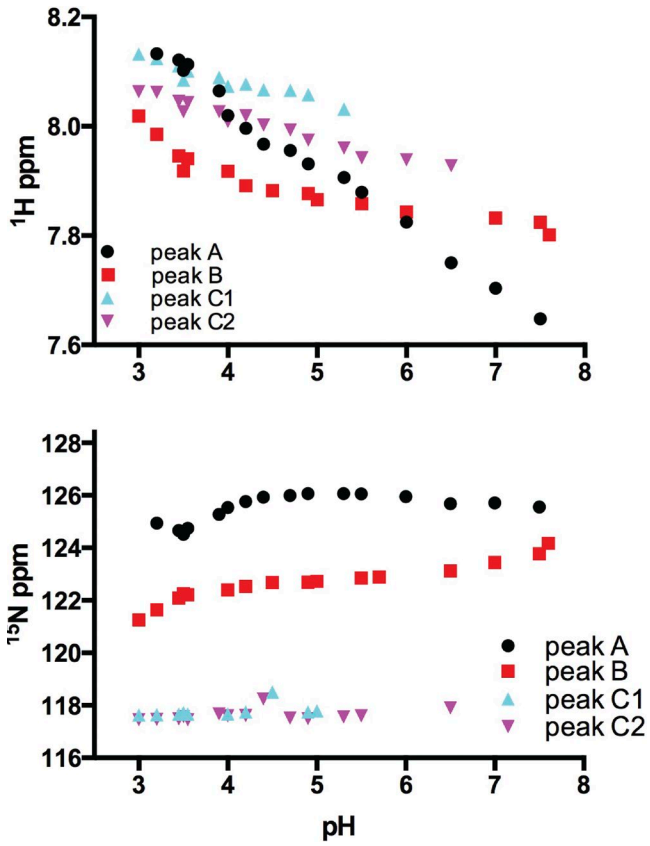

Figure S2. **Chemical shifts of histidine peaks in WT KcsA ΔC.** The plot shows the chemical shift as a function of pH of H124 peaks A, B, C1, and C2 in the ^{1}H dimension (top) and the ^{15}N dimension (bottom).

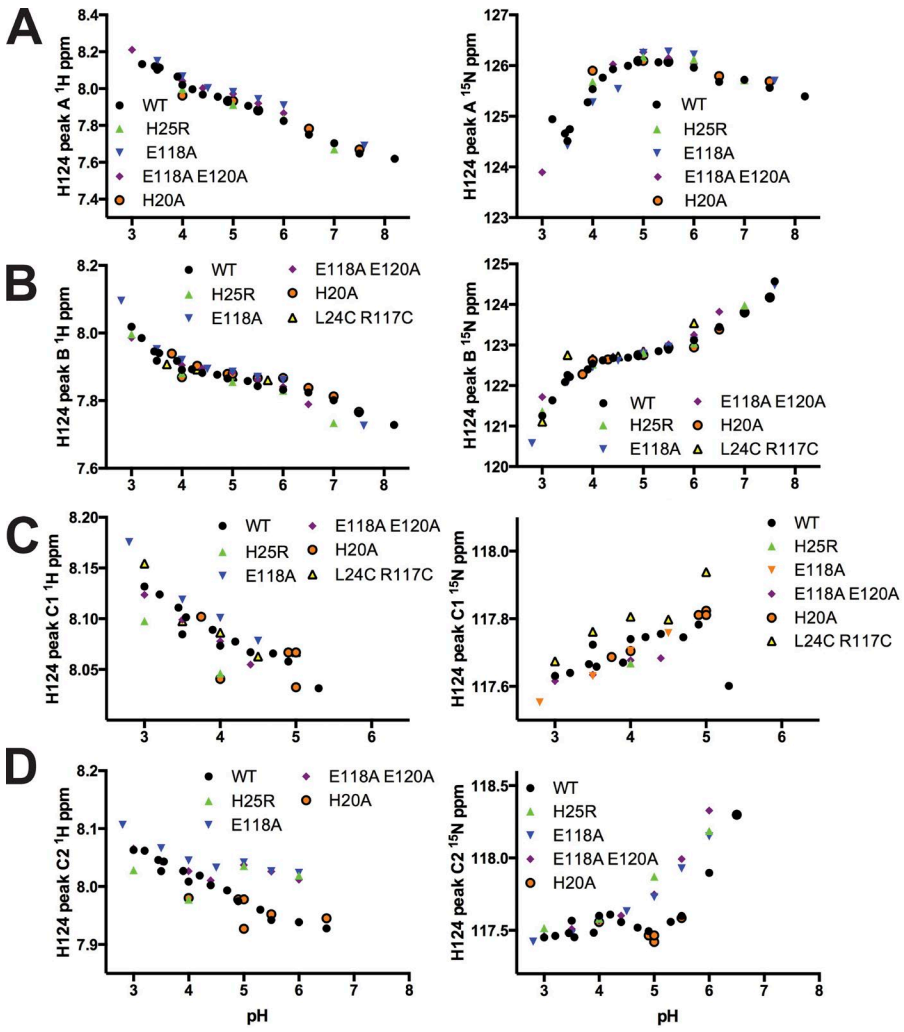

Figure S3. **Comparison of H124 chemical shift pH dependence in various mutants to WT KcsA.** (A–D) Chemical shifts are shown as a function of pH for various mutants in the ^{1}H (left column) and ^{15}N (right column) dimensions for H124 peak A (A), peak B (B), peak C1 (C), and peak C2 (D). KcsA variants include WT, H25R, E118A, E118A E120A, H20A, and L24C R117C.

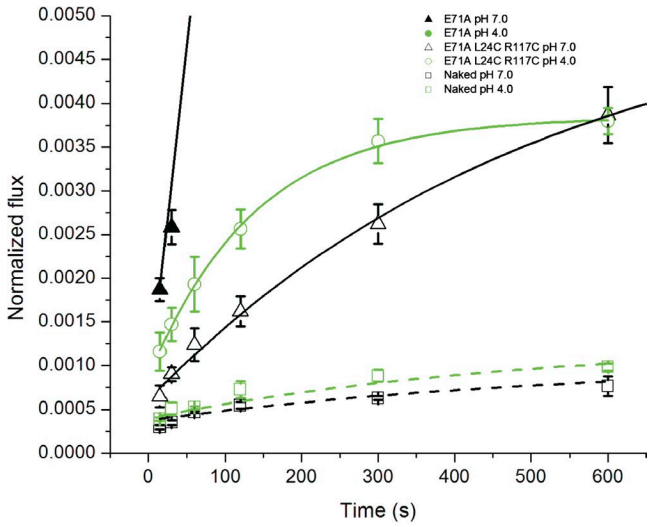

Figure S4. **Detailed view of Rb^+ flux activity of E71A/L24C/R117C.** The graph shows a zoomed-in view of Fig. 4 A with an adjusted y axis for clarity. E71A/L24C/R117C does not show appreciable flux at pH 7.0 and 4.0 compared with the E71A control (black closed triangles). Flux for naked liposomes at pH 7.0 and 4 is included as a control. E71A at pH 4.0 has such high activity that it does not appear on the graph at this scale but is visible in Fig. 4 A.

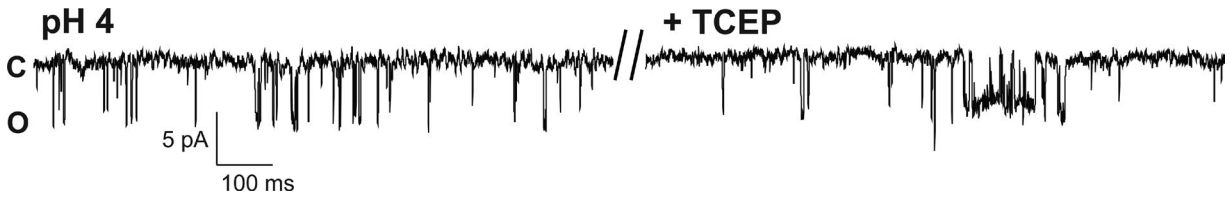

Figure S5. **Example of single channel bilayer recording of L24C R117C KcsA prepared in liposomes without TCEP.** In most instances under these conditions, nothing was observed in the bilayers upon liposome addition. However, in 9 out of ~140 total bilayers, spiky, low Po channels are scouted at 100 mV in pH 4, and upon observation of a channel, 1 mM TCEP in solution at pH 4.0 is perfused into the trans chamber. After 5–10 min of incubation, an increase in Po is observed in channel activity.

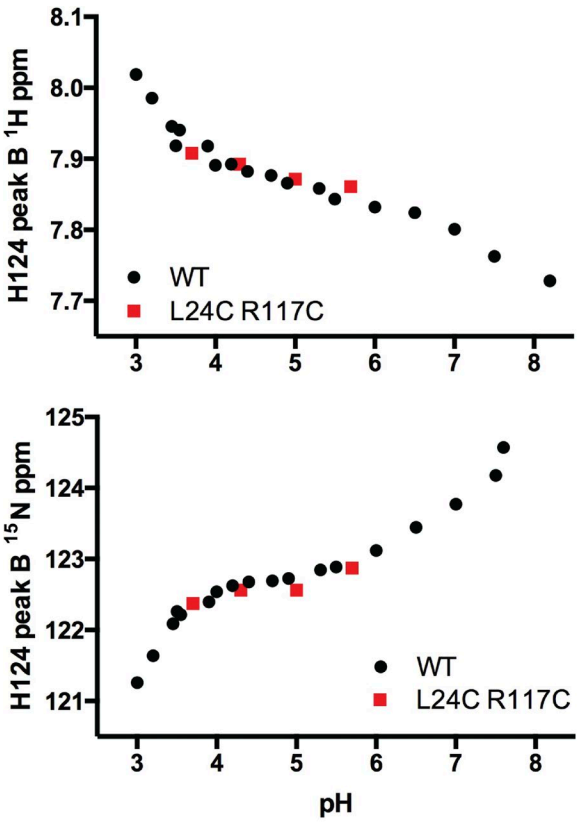

Figure S6. **Chemical shifts of histidine peaks in L24C R117C KcsA ΔC.** Comparison of the chemical shift of H124 peak B in WT and L24C R117C KcsA in the ^{1}H (top) and ^{15}N (bottom) dimensions.

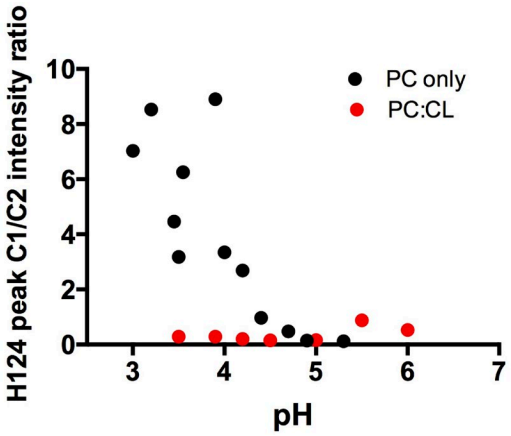

Figure S7. **Intensity ratios for H124 in PC and PC:CL bicelles.** The ratio of H124 peak C1/C2 intensities from [^{1}H,^{15}N]HSQC was calculated and plotted as a function of pH for WT KcsA in PC-only and PC:CL bicelles.

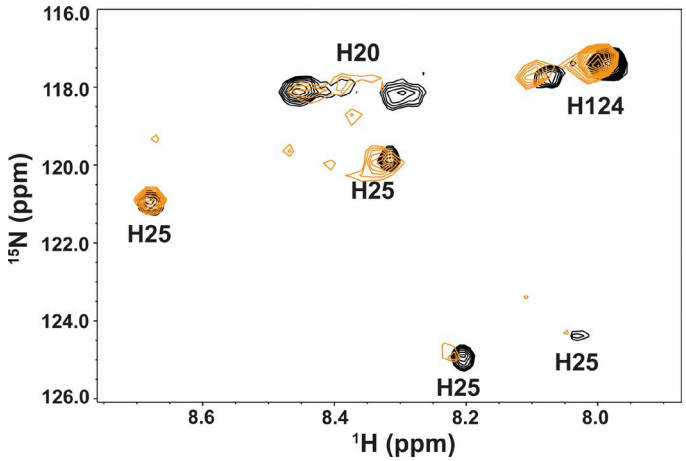

Figure S8. **[^{1}H,^{15}N]HNCA spectrum of KcsA.** The [^{1}H,^{15}N]HNCA spectrum of WT KcsA labeled with [^{13}C,^{15}N]histidine (orange) in PC bicelles was compared with the [^{1}H,^{15}N]HSQC spectrum of [^{15}N]histidine-labeled WT KcsA (black) in PC:CL bicelles at pH 4.2.

Table S1. **Crystallographic data collection and refinement statistics**

Parameter	Value
Data collection	
Wavelength (Å)	0.9792
Space group	I4
Unit cell parameters	
a, b, c (Å)	154.794, 154.794, 74.479
α, β, γ (deg)	90, 90, 90
Resolution range (Å) (Highest shell)	48.95-3.4 (3.52-3.4)
CC(1/2)	99.9 (39.9)
Redundancy	13.26 (13.52)
Completeness (%)	99.8 (99.7)
R_{sym} (%)	15.2 (331.2)
I/sigma(I)	14.16 (1.06)
Refinement	
Resolution	3.4
Number of reflections	12,268 (1,209)
R_{work}/R_{free}	30.79/34.49
Number of atoms	
Protein	4,061
Ligand	4
Water	0
Average B factor (Å^2)	
Protein	42.50
Ligand	15.60
RMSD	
Bond lengths (Å)	0.009
Bond angles (deg)	1.47

Statistics for the highest-resolution shell are shown in parentheses.

Table S2. **Summary of mass spectrometry data**

Peptide sequence	Description	Protease	Modification	Observed m/z of identified ions (<5 ppm)			
				Calculated MH+	2+	3+	4+
1. W.FVGREQERRGH.F	WT - cleaved	chymotrypsin	fully aniline labeled	1,595.84946		532.6213	-
2. W.FVGREQERRGHF.V	WT - not cleaved	chymotrypsin	-	1,517.77104	759.3892	506.59512	380.1983
3. W.FVGCEQERRGH.F	L24C R117C - cleaved	chymotrypsin	fully aniline labeled	1,599.77443	-	-	400.6991
4. W.FVGCEQERRGHF.V	L24C R117C - not cleaved	chymotrypsin	-	1,521.70246	-	507.9052	381.1805
5. K.LLLGRHGSALH.W	WT - cleaved	LysC	-	1,173.68193	587.3446	391.8994	-
6. R.HGSALHWR.A	WT - not cleaved	trypsin	-	963.49047	482.2482	321.8347	-

Rows 1, 2, 5, and 6 refer to analyses performed on WT KcsA, and rows 3 and 4 refer to analyses performed on L24C R117C. Rows 1 and 3 show cleavage at H124, and rows 2 and 4 show cleavage at F125, whereas rows 5 and 6 show cleavage at H25 and R27, respectively. The protease used for in-gel cleavage is noted, as is the use of aniline labeling. The m/z value is the mass-to-charge ratio observed in the spectrum.

REFERENCE

Panchaud, A., J. Hansson, M. Affolter, R. Bel Rhlid, S. Piu, P. Moreillon, and M. Kussmann. 2008. ANIBAL, stable isotope-based quantitative proteomics by aniline and benzoic acid labeling of amino and carboxylic groups. *Mol. Cell. Proteomics*. 7:800–812. http://dx.doi.org/10.1074/mcp.M700216-MCP200